

See discussions, stats, and author profiles for this publication at: <https://www.researchgate.net/publication/233942925>

Anomalous Swelling of Polymer Monolayers by Water Vapor

ARTICLE in MACROMOLECULES · NOVEMBER 2012

Impact Factor: 5.8 · DOI: 10.1021/ma3018553

CITATIONS

5

READS

47

3 AUTHORS, INCLUDING:



Shlomi Medalion

Bar Ilan University

14 PUBLICATIONS 43 CITATIONS

SEE PROFILE



Yitzhak Rabin

Bar Ilan University

172 PUBLICATIONS 3,489 CITATIONS

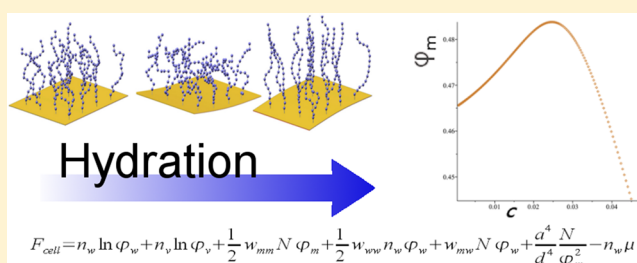
SEE PROFILE

Anomalous Swelling of Polymer Monolayers by Water Vapor

Michal Wagman,* Shlomi Medalion, and Yitzhak Rabin

Department of Physics and Institute of Nanotechnology and Advanced Materials, Bar-Ilan University, Ramat-Gan 52900, Israel

ABSTRACT: A recent experiment showed that when self-assembled monolayers of single-stranded DNA or PNA are exposed to water vapor, they first shrink and then swell with increasing humidity. In order to understand how a monolayer can shrink by absorbing water, we introduce a three-component lattice model consisting of polymer, water, and vacancies. We find that for moderate grafting densities, attractive monomer–water, and repulsive monomer–monomer interactions, at low water vapor concentrations, the adsorption of water is accompanied by enhanced expulsion of vacancies and compression of the monolayer. As humidity is further increased, continued adsorption of water molecules leads to swelling of the monolayer. The low humidity anomaly is predicted to disappear at high grafting densities.



I. INTRODUCTION

In the past few years, a lot of attention has been focused on biosensors, in a microcantilever setup, that are fast, sensitive label-free probes of biochemical recognition reactions, such as DNA-hybridization and high affinity protein–ligand binding, see e.g., refs 1–3 (a more exhaustive list of references can be found in a recent review⁴). The sensor consists of a monolayer of irreversibly grafted biopolymers (DNA or protein molecules), in contact with liquid water reservoir that contains the molecules to be analyzed (e.g., a mixture of complementary and noncomplementary DNA strands), as well as added salt and buffer that control the electrostatic interactions and the pH of the solution. In these experiments, the state of the monolayer is determined by the chemical potential of bulk liquid that depends on the composition of the water + salt + buffer solution. A different experiment, in which the chemical potential of water molecules was directly controlled by changing the concentration of water vapor, was reported in ref 5. Here, the surface stress of a microcantilever with a grafted monolayer of either charged ssDNA or neutral ssPNA was monitored following change of the concentration of water vapor (humidity) in the volume surrounding the cantilever. This experiment produced a number of interesting and unexpected results: (a) Nonmonotonic dependence of the surface stress of the ssDNA-coated cantilever on humidity: while at first, the surface stress increases rapidly with humidity, it then reaches a maximum and decreases with further increase of water vapor concentration. (b) The same behavior was observed for neutral ssPNA molecules (in which the sugar–phosphate backbone was replaced by an amino-acid one), suggesting that this behavior was not of electrostatic origin. (c) Both ssDNA and ssPNA exhibited hysteresis: while nonmonotonic change of surface stress was observed upon increasing humidity, only monotonic increase of the surface stress with decreasing humidity was found. Motivated by the intriguing results of ref 5, in this paper we carry out a mean field

analysis of the response of a grafted polymer monolayer to variations of water vapor concentration in the surrounding reservoir. Since the surface stress can be related to the swelling state of the monolayer⁶ (Figure 1), we derive and analyze the relations between the bulk water vapor concentration (or alternatively, the chemical potential of water molecules) and

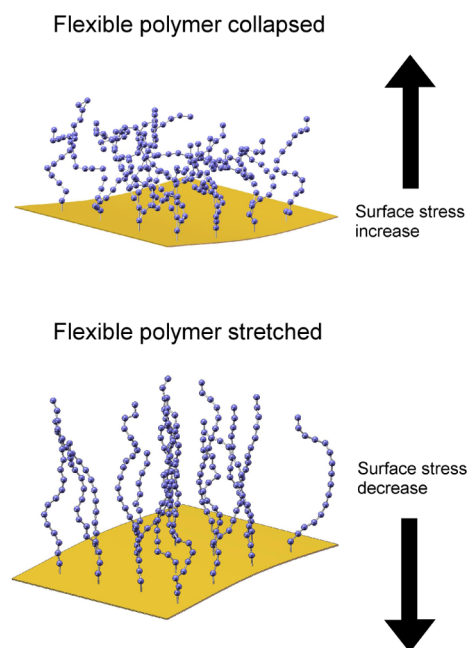


Figure 1. Upper figure shows shrinking of the monolayer which correlates with higher surface stress, Lower figure shows monolayer swelling which correlates with lower surface stress.

Received: September 5, 2012

Revised: November 7, 2012

the monomer concentration inside the brush (or, equivalently, the thickness of the deformable polymer brush).

We begin our analysis with the observation that the initial deswelling of the monolayer as the water vapor concentration is increased, suggests that there are vacancies in the “dry” monolayer and that hydration is accompanied by expulsion of vacancies from the monolayer, in excess of the volume occupied by adsorbed water molecules. In section II, we introduce the three component (polymer+water+vacancies) model of a polymer brush in equilibrium with a water vapor reservoir, and use it to derive the free energy of the system. In section III, we carry out numerical minimization of this free energy and plot the monomer, water and vacancies volume fractions in the brush, as a function of the concentration of water vapor outside it. We find that for physically reasonable choices of interaction parameters (monomer–monomer, monomer–water and water–water) and grafting density, the monomer concentration inside the brush first increases and then decreases with increasing humidity. Finally, in section IV we discuss the connection between our results and experiments on DNA and PNA brushes.

II. THE MODEL

Consider an anchored (e.g., by an end thiol group) self-assembled polymer monolayer, where both vacancies and water are freely exchanged between the layer and a reservoir (water vapor in air). The latter acts as a particle reservoir and a thermal bath which controls the chemical potential of water by changing the concentration of water vapor outside the monolayer. In the following we use a Flory-type lattice model of a polymer brush in which the size of monomers, water molecules and vacancies is assumed to be equal to the lattice spacing a . Since we would like to consider the limit of a dense brush, we have to go beyond the second virial approximation commonly used to describe polymer brushes in the semidilute regime.^{7,8} This can be done using the Flory–Huggins approach to polymer solutions, by introducing the ideal solution entropy contributions of the mobile components (water and vacancies), and adding the entropy cost of stretching the flexible polymer molecules, the mean-field interaction energies between the components, and the free energy change associated with adding water molecules to the monolayer (chemical potential). Below we follow the approach of Lai and Halperin⁹ who discussed the problem of a polymer brush in mixed solvents.

In the following we express all energies and free energies in units of $k_B T$. The free energy per lattice site associated with the combinatorial entropy of the water molecules and of vacancies is given by:

$$-k_B S_{\text{site}} = \varphi_w \ln(\varphi_w) + \varphi_v \ln(\varphi_v) \quad (1)$$

where φ_w and φ_v are the volume fractions of the water and vacancies, respectively, inside the monolayer. There is no direct polymer contribution to this entropy since we assume that the grafted ends of DNA chains are immobile. Using a straightforward extension of the Flory–Huggins mean field theory of polymer solutions¹⁰ to the three component case (polymer, water, and vacancies), we express the interaction energy between components i and j as a product of the corresponding volume fractions φ_i and φ_j :

$$E_{\text{site}} = \frac{1}{2} w_{mm} \varphi_m^2 + \frac{1}{2} w_{ww} \varphi_w^2 + w_{mw} \varphi_m \varphi_w \quad (2)$$

Here w_{mm} , w_{ww} and w_{mw} are effective interaction parameters that represent pairwise interaction energies between adjacent sites occupied by the various components in the system (water–water, water–monomer, and monomer–monomer; interactions with vacant sites were neglected). Note that while in the Flory–Huggins model of polymer solutions all the binary interactions can be absorbed in a single interaction parameter $\chi = w_{mw} - (w_{mm} + w_{ww})/2$, in our ternary system (polymer, water, vacancies/air) three different interaction parameters are needed. In principle, the interaction parameters can be determined from thermodynamic measurements on the corresponding polymer solutions. The elastic entropy cost per polymer, of stretching a polymer chain to a distance $z > aN^{1/2}$ (the rms end to end distance of a Gaussian chain), where N is the number of monomers per chain and z is the height of the monolayer, is

$$F_{\text{el}} = \frac{z^2}{a^2 N}$$

On the average each grafted polymer occupies a cell of volume $V_{\text{cell}} = a^3 N_{\text{sites}} = d^2 z$ where d is the mean spacing between grafting points and n_w and n_v are the number of water molecules and of vacancies, respectively, inside the cell. The number of sites per cell is given by $N_{\text{sites}} = n_w + n_v + N$. Since polymers can stretch and collapse (i.e., z increases or decreases), the volume of the cell can change as well by changing the number of water molecules (n_w) and vacancies (n_v) in it.

In the following we will take the chemical potential of the vacancies to be zero (the number of vacancies is not conserved). The free energy per cell is given by

$$F_{\text{cell}} = N_{\text{sites}}(E_{\text{site}} - k_B S_{\text{site}}) + F_{\text{el}} - n_w \mu \quad (3)$$

Since in equilibrium the chemical potential has the same value inside the brush and in the bulk vapor phase, it can be expressed as

$$\mu(c, T) = \mu_{\text{bulk}}(c, T) = \mu^0(T) + \ln c$$

where c is the bulk concentration of water and the reference chemical potential μ^0 is a function of temperature T only. In order to express the free energy as a function of the variables n_w and n_v we write the volume fractions of the 3 components as

$$\begin{aligned} \varphi_m &= \frac{N}{n_w + n_v + N}; \\ \varphi_w &= \frac{n_w}{n_w + n_v + N}; \\ \varphi_v &= \frac{n_v}{n_w + n_v + N}; \end{aligned} \quad (4)$$

and with the incompressibility constraint, $\varphi_m + \varphi_w + \varphi_v = 1$ we can rewrite eq 3 as

$$\begin{aligned} F_{\text{cell}} &= n_w \ln \left(\frac{n_w}{n_w + n_v + N} \right) + n_v \ln \left(\frac{n_v}{n_w + n_v + N} \right) \\ &+ \frac{1}{2} w_{mm} \frac{N^2}{n_w + n_v + N} + \frac{1}{2} w_{ww} \frac{n_w^2}{n_w + n_v + N} \\ &+ w_{mw} \frac{N n_w}{n_w + n_v + N} + \frac{a^4}{d^4 N} (n_w + n_v + N)^2 - n_w \mu \end{aligned} \quad (5)$$

The number of sites occupied by each specie at equilibrium can be obtained by minimizing this free energy with respect to n_w and n_v

$$\frac{\partial F_{cell}}{\partial n_w} = 0 \quad (6)$$

$$\frac{\partial F_{cell}}{\partial n_v} = 0 \quad (7)$$

III. RESULTS AND ANALYSIS

The parameter that determines the resistance of the grafted polymers to stretching is the surface fraction of grafting sites, $\sigma = (a/d)^2$. Since we are interested in the brush regime in which neighboring polymers strongly overlap ($\sigma > 1/N$), we will consider the cases of intermediate and high grafting densities, $\sigma = 0.25$ and 0.7 , respectively. In order to predict how the state of the brush changes as one varies the chemical potential μ (the control parameter that can be changed by adjusting the water vapor concentration c), we need to specify the values of interaction parameters w_{ij} . The interaction between water molecules is dominated by hydrogen bonding the strength of which is somewhat larger than thermal energy ($1k_B T$) and thus we estimate $w_{ww} = -4.5$.¹¹ The other two parameters depend on the choice of polymer, and since our original goal was to capture the main qualitative features of the observations on ssDNA and ssPNA monolayers reported in ref 5, in principle we should use the thermodynamic values appropriate for these macromolecules. Unfortunately, the corresponding phase diagrams for ssDNA/ssPNA are not available in the literature (note that each DNA length and each base sequence corresponds to a different molecule and the number of such phase diagrams would be prohibitively large). Since water-ssDNA/ssPNA interaction has contributions from both van der Waals attractions and hydrogen bonding, we take the corresponding interaction parameter to be $w_{mw} = -4.5$ as well. The monomer–monomer interactions arise due to a complex interplay between van der Waals attractions, excluded volume repulsions and electrostatic interactions (repulsion between negatively charged phosphates for ssDNA and dipole–dipole interactions between the amino-acids that form the backbone of ssPNA) and we have no obvious way to estimate the corresponding coefficient w_{mm} . As we will show in the following (see, e.g., Figure 5), the anomalous dependence of the swelling of the monolayer with bulk water concentration arises only for sufficient repulsion between monomers and in the following we take $w_{mm} = 1$.

All plots were produced by numerically minimizing the free energy (eq 5) for a given range of μ by means of iteration, using MAPLE. Data for the volume fractions of water molecules, monomers and vacancies was plotted as a function of water vapor concentration, c .

Inspection of Figure 2 shows that for moderate grafting densities, $\sigma = 0.25$, the monomer concentration in the monolayer first increases and then decreases with increasing water vapor concentration outside it. While for low bulk concentrations of water vapor c there are almost no water molecules but there is a considerable volume of vacancies in the polymer brush, in the limit of high bulk water concentration the monolayer becomes fully hydrated and all vacancies are expelled from it (inset in Figure 2). In order to understand the physical origin of this behavior we examine the various

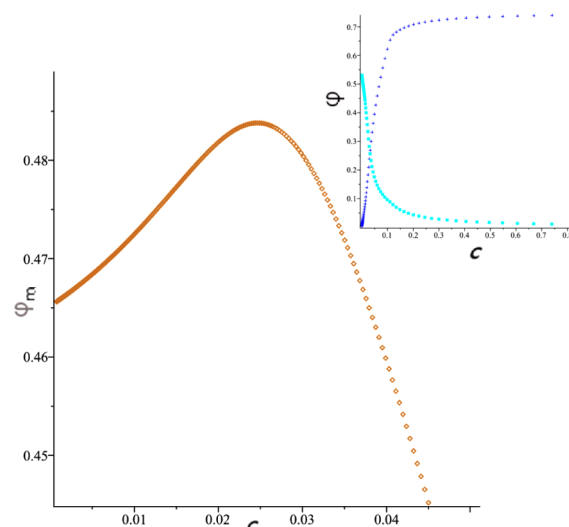


Figure 2. Plots of the monomer volume fraction in the monolayer ϕ_m (gold diamonds), as a function of water vapor concentration c (in arbitrary units), for $\sigma = 0.25$. The corresponding plots for the volume fractions of water molecules ϕ_w (blue crosses) and vacancies ϕ_v (cyan squares) are shown in the inset. The effective interaction coefficients are $w_{mw} = w_{ww} = -4.5$, $w_{mm} = 1$.

contributions to the free energy in eq 5 (Figure 3). At small concentrations in the bulk, the water concentration inside the

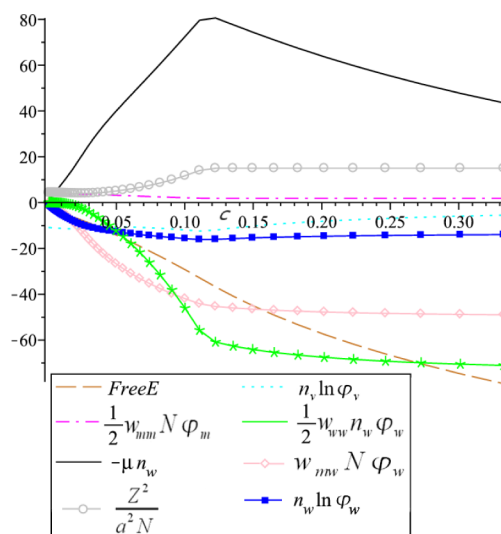


Figure 3. Plots of the various components contribution to the free energy, as a function of water vapor concentration c (in arbitrary units) for $\sigma = 0.25$. Total free energy (dashed gold line), water–water interaction (green asterisks), combinatorial entropy of vacancies (cyan dots), chemical potential contribution (black line), combinatorial entropy of water (blue solid boxes), elastic free energy (gray circles), monomer–monomer interaction (magenta dash-dot), and monomer–water interaction (pink diamonds).

monolayer is negligible and the state of the monolayer is determined by the interplay of 3 contributions: repulsive monomer–monomer interactions and entropy of vacancies both of which tend to swell the “dry” monolayer and elastic restoring forces which oppose swelling of the monolayer. Since for moderate grafting densities the restoring elastic forces are relatively weak, the equilibrium dry brush contains a large number of vacancies (ϕ_v approaches 0.55 as $c \rightarrow 0$; see inset in

Figure 2) and is stretched with respect to the vacancy-free state. As μ increases further and water begins to enter the monolayer, monomer–water attraction and entropy of water terms come into play (see Figure 3) and the concentration of vacancies begins to decrease. Since the monomer–water attraction is proportional to the product $\phi_m \phi_w$, free energy is minimized by increasing both ϕ_w and ϕ_m , i.e., by simultaneously absorbing water and increasing the monomer concentration in the monolayer by expelling the vacancies and shrinking. Eventually, as all vacancies are expelled, further intake of water must be accompanied by swelling of the monolayer, as indeed observed in Figure 2. The above mechanism suggests that since at high grafting densities the volume fraction of vacancies in the dry monolayer is expected to be small (and correspondingly, the monomer volume fraction is high), there will be no initial stage in which the monomer concentration increases with increasing water vapor concentration and only continuous swelling of the monolayer will be observed. These expectations are confirmed by the results of calculations shown Figure 4 where we plot the monomer, vacancies and water volume fractions as a function of water vapor concentration, for $\sigma = 0.7$.

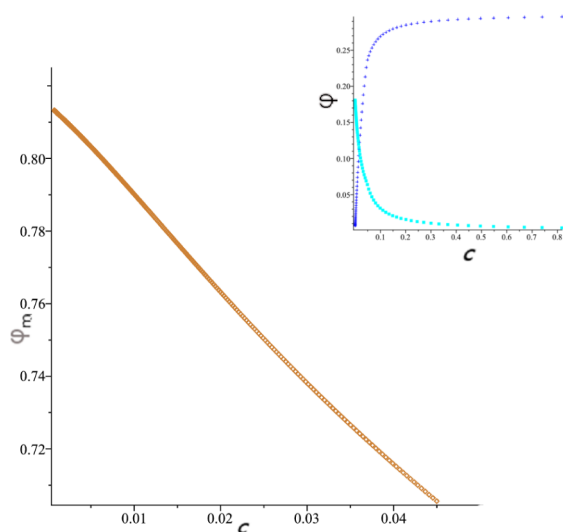


Figure 4. Plots of the monomer volume fraction in the monolayer ϕ_m (gold diamonds), as a function of water vapor concentration c (in arbitrary units) for $\sigma = 0.7$. The corresponding plots for the volume fractions of water molecules ϕ_w (blue crosses) and vacancies ϕ_v (cyan squares) are shown in the inset. The effective interaction coefficients are $w_{mw} = w_{ww} = -4.5$, $w_{mm} = 1$.

Note that according to our model, the swelling anomaly is a direct consequence of monomer–monomer repulsion in the dry state; if we were to replace these repulsions by attractions (negative w_{mm}) the dry monolayer would not contain enough vacancies to produce the initial increase in monomer concentration (decrease of the thickness of the monolayer) with increasing water vapor concentration outside it. This expectation is confirmed in Figure 5 where we plotted the volume fractions of all the components as a function of water vapor concentration for $w_{mm} = -1$ and $\sigma = 0.25$; the layer swells monotonically with increasing humidity through the entire range of water concentration.

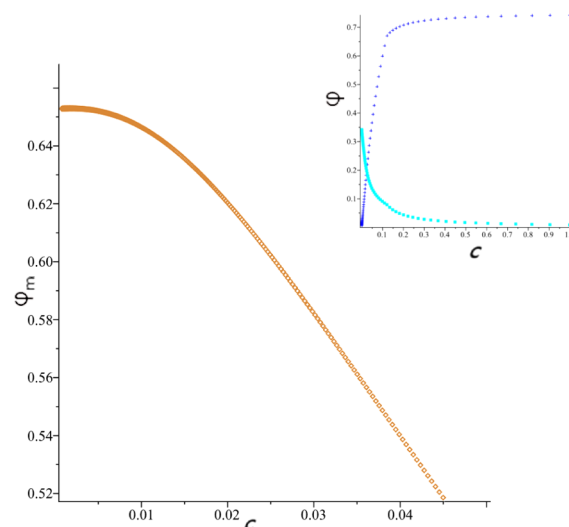


Figure 5. Plot of the monomer volume fraction in the monolayer ϕ_m (gold diamonds), as a function of water vapor concentration c (in arbitrary units) for $w_{mm} = -1$. The corresponding plot for the volume fractions of water molecules ϕ_w (blue crosses) and vacancies ϕ_v (cyan squares) is shown in the inset. Other parameters are $\sigma = 0.25$ and $w_{mw} = w_{ww} = -4.5$.

IV. DISCUSSION

In this work, we analyzed a mean-field lattice model of swelling of a monolayer of grafted polymer chains, due to adsorption of water molecules from the gas phase. In order to reproduce, albeit qualitatively, the observation⁵ that a monolayer of ssDNA or ssPNA molecules grafted to a gold surface first contracts and then expands upon increasing humidity, we allowed for the presence of vacancies in the monolayer. Since no qualitative differences between charged ssDNA and neutral ssPNA were observed in the above experiments, in this work we focused on brushes of neutral polymer chains. Qualitatively similar results were obtained for charged brushes in which we incorporated the counterion entropy that dominates the electrostatics of a polyelectrolyte brush in the absence of salt¹² (not shown). We found that for moderate grafting densities, the combination of attractive monomer–water and repulsive monomer–monomer interactions results in nonmonotonic dependence of the monomer concentration (or alternatively, of the thickness of the monolayer) on water vapor concentration: while initially the monomer volume fraction increases (and the layer shrinks) with increasing humidity, it reaches a maximum and then decreases as humidity is increased further. The above trends concur with the observations of ref 5, in which similar nonmonotonic behavior was observed when humidity was increased. However, the experimenters also reported the observation of hysteresis: when humidity was subsequently decreased, the monomer concentration increased monotonically with decreasing water vapor concentration. Clearly, since the experiments were carried out under nonequilibrium conditions (relative humidity was changed at a rate of 1% per minute), the observed hysteresis can not be captured by our equilibrium approach and we can only speculate about its origin. One possibility is that the removal of water molecules from the vicinity of ssDNA molecules upon decreasing humidity, involves overcoming significant free energy barriers and therefore ssDNA remains hydrated through much of the drying process. If the interaction between hydrated ssDNA

molecules is attractive (e.g., due to hydrophobic interactions), our model predicts that the monolayer will deswell monotonically with decreasing vapor concentration, in agreement with experiment. Another possibility is that the slow nonequilibrium kinetics observed in the experiments of ref 5 is the result of lateral phase separation due to slow diffusion of thiol head groups on the gold surface,¹³ making the monolayer density nonhomogenous.

Finally, apart from providing a theoretical framework for interpreting the experimental results of ref 5, our model predicts that the initial deswelling upon increasing humidity should disappear for sufficiently high polymer grafting densities. This concurs with preliminary experimental results on dense ssDNA monolayers and further experiments are in progress.¹⁴

AUTHOR INFORMATION

Notes

The authors declare no competing financial interest.

ACKNOWLEDGMENTS

Y.R. would like to acknowledge helpful correspondence with J. Tamayo and M. Calleja. This work was supported by a grant from the US–Israel Binational Science Foundation.

REFERENCES

- (1) Fritz, J.; Baller, M. K.; Lang, H. P.; Rothuizen, H.; Vettiger, P.; Meyer, E.; Gerber, Ch; Gimzewski, J. K. *Science* **2000**, 288, 316–318.
- (2) Guanghua, W.; Haifeng, J.; Hansen, K.; Thundat, T.; Datar, R.; Cote, R.; Hagan, M. F.; Chakraborty, A. K.; Majumdar, A. *Proc. Natl. Acad. Sci. U.S.A.* **2001**, 98, 1560–1564.
- (3) McKendry, R.; Jiayun, Z.; Arntz, Y.; Strunz, T.; Hegner, M.; Lang, H. P.; Baller, M. K.; Certa, U.; Meyer, E.; Gutherodt, H.-J.; Gerber, C.; et al. *Proc. Natl. Acad. Sci. U.S.A.* **2002**, 99, 9783–9788.
- (4) Zhang, N. H.; Tan, Z. Q.; Li, J. J.; Meng, W. L.; Xu, L. W. *Curr. Opin. Colloid Interface Sci.* **2011**, 16, 592–596.
- (5) Mertens, J.; Rogero, C.; Calleja, M.; Ramos, D.; Martin-Gago, J. A.; Briones, C.; Tamayo, J. *Nature Nanotechnol.* **2008**, 3, 301–307.
- (6) Utz, M.; Begley, M. R. *J. Mech. Phys. Solids* **2008**, 56, 801–814.
- (7) Alexander, S. J. *Phys. Paris* **1977**, 38, 983–987.
- (8) De Gennes, P. G. *J. Phys. Paris* **1976**, 37, 1445–1452.
- (9) Lai, P.-Y.; Halperin, A. *Macromolecules* **1992**, 25, 6693–6695.
- (10) Rubinstein, M.; Colby, R.H., *Polymer Physics*; Oxford University Press: Oxford, U.K., 2003.
- (11) Arunan, E.; Desiraju, G. R.; Klein, R. A.; Sadlej, J.; Scheiner, S.; Alkorta, I.; Clary, D. C.; Crabtree, R. H.; Dannenberg, J. J.; Hobza, P.; Kjaergaard, H. G.; Legon, A. C.; Mennucci, B.; Nesbitt, D. J. *Pure Appl. Chem.* **2011**, 83, 1637–1641.
- (12) Pincus, P. *Macromolecules* **1991**, 24, 2912–2919.
- (13) Sheehan, P. E.; Whitman, L. J. *Phys. Rev. Lett.* **2002**, 88, 156104.
- (14) Tamayo, J. Private communication.